AAS 22-691

FAST APPROXIMATION OF CONTINUOUS THRUST OPTIMAL RELATIVE CONTROL IN THE THREE BODY PROBLEM

Jackson Kulik[*], **William Clark**[†], **and Dmitry Savransky** [‡]

Using first and second order variational equations as well as cocycle properties associated with an indirect optimal control problem, we may precompute and interpolate state transition tensors about a given reference trajectory of a dynamical system. We apply this to the approximate solution of continuous thrust optimal control of satellite relative motion in the three body problem. Arbitrary relative transfers near some reference orbit are approximated without requiring numerical integration each time the boundary conditions or their timing are adjusted. This approach enables fast computation in trajectory and mission design.

INTRODUCTION

Trajectory and mission design problems often require nested optimizations to determine optimal trajectories that balance mission goals with operational constraints. For example, Refs. 1, 2 deal with doubly nested optimizations of formation flight behavior to determine the optimal observation schedule that maximizes science yield while minimizing control costs for coordinated flight of a telescope and starshade in Sun-Earth space. In order to meet these objectives, a traveling salesman type problem is posed to determine which stars to observe and on what schedule. A proposed itinerary is judged partially on the basis of the fuel costs to maneuver the starshade accordingly. The fuel cost for one leg of the journey may be assessed by solving a continuous thrust optimal control problem. Thus, computation of multiple continuous thrust optimal control problems is just one step in evaluating the objective function for one proposed itinerary when considering the overall scheduling problem. Fast algorithms to solve continuous thrust optimal relative control problems in the three body problem are necessary to facilitate solution of nested optimization problems.

The continuous thrust optimal control of one satellite relative to another has been extensively studied in the context of the two body problem.[3–9] These methods generally rely on the analytical form of the state transition matrix solutions to the Clohessy-Wiltshire or Tschauner-Hempel equations which are not available in the context of the three body problem. On the other hand, relative impulsive control of formations in the three body problem has also been well studied[10–13] with some recent advances in continuous optimal control. Franzini et al.[14] examined continuous thrust control applied to relative motion in the elliptical three body problem using an adjoint method. While this methodology improves fidelity and speed of computation, numerical integration is still required each time a new optimal control problem is posed and may be unsuited for applications in which high computational speed of this subproblem is required to render some overarching problem

[*]PhD Student, Center for Applied Mathematics, Cornell University, Ithaca, NY, 14850. jpk258@cornell.edu
[†]Visiting Assistant Professor, Mathematics, Cornell University, Ithaca, NY, 14850.
[‡]Associate Professor, Mechanical and Aerospace Engineering, Cornell University, Ithaca, NY, 14850.

tractable. Next, a method using generating functions to solve optimal continuous thrust rendezvous problems generalizes well for use in the three body problem where no analytical form of the state transition matrix is known.[15] While this approach allows for solution of the problem with arbitrary boundary conditions after a single computation of the generating function, the generating function must be recomputed from scratch whenever the time of flight or initial epoch of the problem is adjusted. Similarly, Boone et al.[16] achieved solution of low thrust problems by differential dynamic programming with state transition tensors to obtain feedback control laws for arbitrary motion near a reference orbit and over a specified time of flight. Their more recent work on impulsive maneuvers has allowed for this method to be extended to not just calculate for a single time of flight, but a neighborhood of time of flight using one of two methods that store temporal derivatives or use Taylor approximations in time.[17,18] However, these methods still do not work for arbitrary initial epoch and arbitrary time of flight outside of some small region.

We aim to approximately solve continuous thrust optimal relative control problems with arbitrary initial epoch, time of flight, and boundary conditions without performing numerical integration online. We also seek to limit storage requirements from precomputed data, and to obtain fitness metrics related to fuel use without numerical integration. In order to accomplish these goals, we begin by reviewing the properties of the first and second order variational equations. From there, we will formulate a basic optimal control problem. Finally, we outline an algorithm to precompute and interpolate variational data associated with a reference trajectory in the dynamical system of states and costates. The linear variational data yields initial costates which approximately solve the optimal control problem after only a few matrix products and the solution of a linear system twice the size of the initial state space. The second order variational data then allows for approximation of metrics related to fuel use with another product involving the state transition tensor. Additionally, the second order variational data may be used in a Newton iteration scheme to find more accurate solutions of the optimal control problem than would be available with just the linear variational information. Examples of motion around a reference halo orbit are used to evaluate the approximation error for these approaches in a rendezvous setting. A similar approach to precomputation and interpolation was taken by the authors in a previous work considering only impulsive maneuvers applied to the relative motion dynamics of a space-telescope working in conjunction with a starshade.[19]

VARIATIONAL EQUATIONS

The first and second order variational equations associated with a dynamical system are derived in Ref. 20. The notion of state transition tensors is also explored in Refs. 21, 22. We will describe commonly known properties of the state transition matrix in both matrix and component form to build intuition for properties of the second order variational state transition tensor which is most clearly described in component form.

Given an autonomous dynamical system in $\mathbb{R}^n$, the state vector $\mathbf{x}$ evolves according to the system of ordinary differential equations

$$\frac{d}{dt}\mathbf{x} = \mathbf{F}(\mathbf{x}) \tag{1}$$

The associated flow map is defined such that

$$\frac{d}{dt}\varphi_t(\mathbf{x}) = \mathbf{F}(\varphi_t(\mathbf{x})), \quad \varphi_0(\mathbf{x}) = \mathbf{x} \tag{2}$$

The flow map possesses the semigroup property in time

$$\varphi_t \circ \varphi_s = \varphi_{t+s} \tag{3}$$

The Jacobian of the flow map yields the state transition matrix (STM) $\Phi(t,0)$ associated with a given flow from time 0 to time t. We adopt indexing for the state transition matrix rows i and columns j

$$\Phi^i_j(t,0) = \frac{\partial \varphi^i_t(\mathbf{x})}{\partial x_j} \tag{4}$$

where the upper index i of the flow map refers to the ith component of the output. Exchanging the order of temporal and spatial derivatives (assuming F has continuous spatial derivatives) then applying chain rule yields the n^2 first order variational equations

$$\frac{d\Phi(t,0)}{dt} = \frac{\partial \mathbf{F}(\mathbf{x})}{\partial \mathbf{x}}\Phi(t,0), \quad \Phi(0,0) = I_n \tag{5}$$

where I_n gives the n by n identity matrix. Or in components where summation with respect to l is understood and $\delta_{i,j}$ is the Kronecker delta

$$\frac{d\Phi^i_j(t,0)}{dt} = \frac{\partial F_i(\mathbf{x})}{\partial x_l}\Phi^l_j(t,0), \quad \Phi^i_j(0,0) = \delta_{i,j} \tag{6}$$

The cocycle property is most recognizable in matrix form and stems from application of the chain rule to the semigroup property.

$$\Phi(t_2,t_0) = \Phi(t_2,t_1)\Phi(t_1,t_0) \tag{7}$$

or in components

$$\Phi^i_j(t_2,t_0) = \Phi^i_l(t_2,t_1)\Phi^l_j(t_1,t_0) \tag{8}$$

Note that the given relationship is not commutative. Moving on to the second order variational equations, we define the second order (2,1)-state transition tensor (STT) $\Psi(t,0)$

$$\Psi^i_{j,k}(t,0) = \frac{\partial^2 \varphi^i_t(\mathbf{x})}{\partial x_j \partial x_k} \tag{9}$$

Applying the product rule to equation 6, we find that the n^3 equations in equation 10 depend not only on the values of Ψ but also Φ

$$\frac{d\Psi^i_{j,k}(t,0)}{dt} = \frac{\partial^2 F_i(\mathbf{x})}{\partial x_l \partial x_q}\Phi^l_j(t,0)\Phi^q_k(t,0) + \frac{\partial F_i(\mathbf{x})}{\partial x_l}\Psi^l_{j,k}(t,0), \quad \Psi^i_{j,k}(0,0) = 0 \tag{10}$$

The second order generalization to the cocycle conditions come from differentiating equation 8

$$\Psi^i_{j,k}(t_2,t_0) = \Psi^i_{l,k}(t_2,t_1)\Phi^l_j(t_1,t_0) + \Phi^i_l(t_2,t_1)\Psi^l_{j,k}(t_1,t_0) \tag{11}$$

A second order approximation of a perturbation to the flow map is given by a truncated Taylor series:

$$\varphi^i_t(\mathbf{x}+\delta\mathbf{x}) \approx \varphi^i_t(\mathbf{x}) + \Phi^i_j(t,0)\delta x^j + \frac{1}{2}\Psi^i_{jk}(t,0)\delta x^j \delta x^k \tag{12}$$

We have summarized the variational machinery necessary for our approximation algorithm. Next, we define the optimal control problem to which we will apply analysis of variational equations.

OPTIMAL CONTROL PROBLEM

We examine the energy optimal unconstrained thrust problem as outlined in.[1,23] While energy is not the most applicable metric for fuel use, this problem is more tractable for treatment with variational equations than the fuel optimal and bounded thrust problems which possess discontinuous derivatives in the mass or costate equations stemming from the switching function in the bang-bang control.[23]

The governing dynamical system without control is given by equation 1. We seek to satisfy twelve boundary conditions on the initial and final states which are each six dimensional vectors consisting of three dimensional position and velocity $\mathbf{x} = [\mathbf{r}^T \quad \mathbf{v}^T]^T$

$$\mathbf{x}(t_0) = \mathbf{x_0}, \quad \mathbf{x}(t_f) = \mathbf{x_f} \tag{13}$$

Simultaneously, we seek to minimize the quadratic integral in the control vector $\mathbf{u}$

$$J = \int_{t_0}^{t_f} \frac{1}{2}\mathbf{u}^T\mathbf{u}\,\mathrm{d}t \tag{14}$$

The Hamiltonian corresponding to this problem and the dynamical system given by equation 1 is

$$H = \frac{1}{2}\mathbf{u}^T\mathbf{u} + \boldsymbol{\lambda}^T\mathbf{F} + \mathbf{p}^T\mathbf{u} \tag{15}$$

where $\boldsymbol{\lambda}$ is a six dimensional collection of costates and $\mathbf{p} = (\lambda_4, \lambda_5, \lambda_6)^T$. The resulting system of twelve ordinary differential equations is given by equation 1 and

$$\frac{d}{dt}\boldsymbol{\lambda} = -\left(\frac{\partial \mathbf{F}(\mathbf{x})}{\partial \mathbf{x}}\right)^T \boldsymbol{\lambda} \tag{16}$$

A two point boundary value problem arises from equations 1 and 16 along with the boundary conditions from equation 13. Solution of this system yields the optimal control effort $\mathbf{u} = -\mathbf{p}$ as a function of the initial costates after integration of the system. From these, equation 14 can be integrated and the performance metric can be evaluated. Typically, repeated numerical integration as a part of a shooting method is required for the solution of this indirect optimal control problem. Note that the solution of the two point boundary value problem gives only necessary conditions for an optimal trajectory and that sufficient conditions of optimality require the generalized Legendre–Clebsch condition also be satisfied along the trajectory

$$\frac{\partial^2 H}{\partial u^2} > 0 \tag{17}$$

We attempt to perform numerical integration of variational equations ahead of time to avoid numerical integration each time a new optimal control problem needs to be solved online. By using the variational equations, we assume that our optimal control occurs in a neighborhood of some reference trajectory.

APPROXIMATE OPTIMAL RELATIVE CONTROL

Assume an uncontrolled reference trajectory with initial conditions $\mathbf{x}(0) = \mathbf{x}_0$, following the dynamics given in equation 1 until it reaches state $\mathbf{x}(t_f) = \mathbf{x}_f$ at some final time t_f. This reference

trajectory represents the natural motion of some chief satellite under a given set of dynamics. We are interested in controlling another nearby deputy satellite with initial state $\mathbf{x}_0 + \delta\mathbf{x}_0$, so that it arrives at the final desired state $\mathbf{x}_f + \delta\mathbf{x}_f$ at some time t_f. $\delta\mathbf{x}(t)$ is the relative state at time t and gives the difference in state between the deputy and chief satellite states.

We now turn to the approximation of solutions to our optimal control problem and the performance metric. Consider the augmented state vectors for the reference trajectory

$$\mathbf{y} = [\mathbf{x}^T \quad \boldsymbol{\lambda}^T]^T, \quad \mathbf{z} = [\mathbf{x}^T \quad \boldsymbol{\lambda}^T \quad J]^T \tag{18}$$

We may calculate the solutions to the first and second order variational equations as described in section 1, applied to the augmented system for $\mathbf{z}$

$$\frac{d}{dt}\mathbf{z} = \mathbf{G}(\mathbf{z}) = \left[\left(\mathbf{F}(\mathbf{x})^T + \begin{bmatrix}\mathbf{0} & \mathbf{u}^T\end{bmatrix}\right) \quad -\boldsymbol{\lambda}^T\left(\frac{\partial \mathbf{F}(\mathbf{x})}{\partial \mathbf{x}}\right) \quad \frac{1}{2}\mathbf{u}^T\mathbf{u}\right]^T \tag{19}$$

In particular, the variational equations can be solved about the reference trajectory without control applied. In this case, the initial costates are all set to zero ($\boldsymbol{\lambda}_0 = \mathbf{0}$). The resulting state transition matrix Φ and tensor Ψ can be used to approximately describe natural and optimally controlled motion in the vicinity of the reference trajectory. The optimal control problem of relative motion given a specified initial relative state $\delta\mathbf{x}_0$ and final relative state $\delta\mathbf{x}_f$ can then be solved up to first order in the following manner:

$$\delta\boldsymbol{\lambda}_0 \approx \left(\Phi^{\mathbf{x}}_{\boldsymbol{\lambda}}(t_f, t_0)\right)^{-1}\left(\delta\mathbf{x}_f - \Phi^{\mathbf{x}}_{\mathbf{x}}(t_f, t_0)\delta\mathbf{x}_0\right) \tag{20}$$

where

$$\Phi^{\mathbf{a}}_{\mathbf{b}}(t_f, t_0) = \frac{\partial \mathbf{a}(t_f)}{\partial \mathbf{b}(t_0)} \tag{21}$$

However, the performance metric $J(t_f) = J_f$ cannot be approximated by the first order variational equations given that it is defined by a quadratic term (it can be approximated, but only trivially as zero). For this, we require the second order variational equations:

$$J_f \approx \Psi^{J}_{\boldsymbol{y},\boldsymbol{y}}(t_0, t_f)\delta\mathbf{y}_0\delta\mathbf{y}_0 \tag{22}$$

with

$$\Psi^{\mathbf{a}}_{\mathbf{b},\mathbf{c}}(t_f, t_0) = \frac{\partial^2 \mathbf{a}(t_f)}{\partial \mathbf{b}(t_0)\partial \mathbf{c}(t_0)} \tag{23}$$

Additionally, we may improve the approximation of $\delta\boldsymbol{\lambda}_0$ from equation 20 by using Newton's method to numerically solve equation 24 for $\delta\boldsymbol{\lambda}_0$ given $\delta\mathbf{x}_0$ and $\delta\mathbf{x}_f$:

$$\delta\mathbf{x}_f \approx \Phi^{\mathbf{x}}_{\mathbf{y}}\delta\mathbf{y}_0 + \Psi^{\mathbf{x}}_{\mathbf{y},\mathbf{y}}\delta\mathbf{y}_0\delta\mathbf{y}_0 \tag{24}$$

where the Jacobian $\Phi^{\mathbf{x}}_{\boldsymbol{\lambda}}$ is used as the derivative in the Newton iteration scheme.

Note that the reference trajectory is trivially the globally optimal solution of the energy minimal control problem with boundary conditions $\mathbf{x}(0) = \mathbf{x}_0$ and $\mathbf{x}(t_f) = \mathbf{x}_f$ given that it satisifies the

boundary conditions without any control effort. The generalized Legendre–Clebsch condition is satisfied along the reference trajectory, and further, $\frac{\partial^2 H}{\partial u^2} > 0$ on a neighborhood around the reference trajectory. For sufficiently small $\delta \mathbf{x}_0$ and $\delta \mathbf{x}_f$ as well as nonsingular $\Phi^{\mathbf{x}}_{\boldsymbol{\lambda}}(t_f, t_0)$, the generalized Legendre–Clebsch condition will also be satisfied along the controlled deputy satellite trajectory, ensuring that the control is a local minimum for the cost function in equation 14.

In this manner, we can approximately solve any relative optimal control problem with arbitrary boundary conditions sufficiently close to a reference orbit given a fixed initial epoch and time of flight for the reference trajectory. So far, this puts the proposed methodology on roughly equal footing with that of Refs. 15, 16 in terms of computational efficiency, but without the ability to determine closed loop optimal control laws or to increase the order of the approximation arbitrarily.

PRECOMPUTATION OF VARIATIONAL DATA

In order to expand our methodology to solve optimal relative control problems with arbitrary boundary conditions as well as arbitrary initial epoch and time of flight along a reference orbit, we turn to cocycle conditions and develop a methodology to interpolate variational data.

We detail an algorithm consisting of a precomputation and storage phase, along with a second online phase in which specific optimal control problems are solved. The precomputation assumes a given reference orbit, specified by initial conditions as well as a time range. For a periodic orbit, the time range can be assumed infinite. A discretization size of 2^m given $m \in \mathbb{N}$ is chosen and the time range or period is broken into 2^m intervals of equal length. Along each interval, the reference trjectory variational equations are integrated, and the first and second order state transition tensors $\Phi(\Delta_{m,j}), \Psi(\Delta_{m,j})$ along the intervals $\Delta_{m,j}$ are stored with

$$\Delta_{m,j} = \left(T_0 + \frac{T_f - T_0}{2^m} j, T_0 + \frac{T_f - T_0}{2^m}(j+1) \right) \tag{25}$$

where T_0 and T_f give the initial and final epochs of the reference trajectory under consideration. For a periodic orbit T_0 is assumed to be zero, and T_f is the period of the orbit.

The cocycle property and generalized cocycle property in equations 8 and 11 can be used to calculate and store $\Phi(\Delta_{i,j}), \Psi(\Delta_{i,j})$ for decreasing values of i from $m-1$ to 0. This yields precomputed variational data at $m+1$ different levels of discretization, all the way from our original finest discretization on up to state transition tensors for the entire reference trajectory (or periodic orbit) at $i = 0$. Figure 1 demonstrated the multi-level discretization of a periodic orbit. This concludes the precomputation step of the algorithm which requires approximately $2^{m+1}(2n)^2$ floating point entries of data to be stored for the first order state transition tensor, an additional $2^{m+1}(2n)^2$ entries for the second order sensitivity of the performance metric J, and optionally $2^{m+1}(2n)^3$ entries for $\Psi^{\mathbf{y}}_{\mathbf{y}}$ where n is the dimension of the state variables and $2n$ is the dimensions of the combined states and costates. For a very fine discretization ($m = 11$ giving finer than tenth of a day precision on a six month Sun-Earth L2 Halo orbit), and storage of all first and second order variational information in double precision format, storage requirements amount to approximately 66 megabytes which fits manageably within the RAM of a modern desktop computer. Cutting second order variational information that does not pertain to fuel usage, and reducing to single day discretization leads to memory usage on the order of only a single megabyte. In the future, a method of storing sparse directional variational data rather than the whole variational system could cut storage requirements by orders of magnitude at some cost to accuracy.[24] A Fourier representation of the variational data

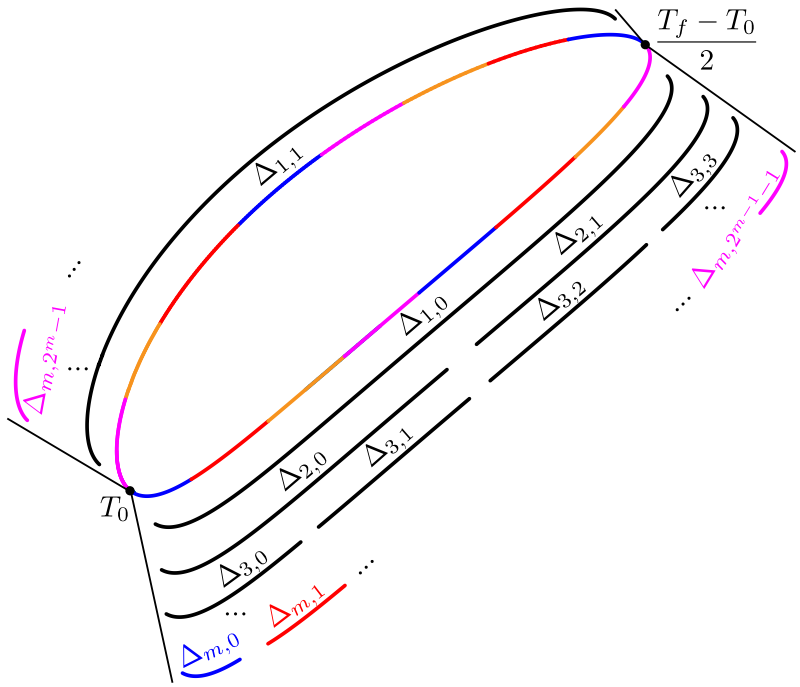

Figure 1: A notional multi-level discretization of a periodic orbit with the halfway point in time labeled. $\Delta_{i,j}$ is shown for various indices along the first half of the orbit up to the mth level of discretization.

along a periodic orbit may also be a possible way to reduce storage costs though we do not explore that further here.[25]

For the online stage of the algorithm, many optimal relative control problems may be solved in succession. Given arbitrary t_0, t_f in the time range corresponding to the precomputed reference trajectory, $\Phi(t_f, t_0), \Psi(t_f, t_0)$ are computed with the cocycle conditions by piecing together precomputed state transition tensors.

Specifically, the lowest index i^* is found where there exists j^* such that $\Delta_{i^*,j^*} \subseteq (t_0, t_f)$. From here, the process is repeated on the left and right disconnected portions of the original interval with the inner interval removed, $(t_0, t_f) \setminus \Delta_{i^*,j^*}$. A running approximation of the state transition tensors is kept using the cocycle conditions. This continues until $i = m$, at which point $\mathcal{O}(m)$ operations have taken place and the state transition tensors approximations are $\Phi(t'_f, t'_0), \Psi(t'_f, t'_0)$ where $0 \leq t'_0 - t_0, t_f - t'_f \leq (T_f - T_0)2^{-m}$.

We approximate $\Phi(t'_0, t_0), \Psi(t'_0, t_0)$ as well as $\Phi(t_f, t'_f), \Psi(t_f, t'_f)$ and then use the cocycle conditions to augment $\Phi(t'_f, t'_0), \Psi(t'_f, t'_0)$ and come up with our final approximation of $\Phi(t_f, t_0), \Psi(t_f, t_0)$.

Let $(a, b) \subseteq \Delta_{m,j}$, then entrywise linear interpolants are given by

$$\Phi(b, a) \approx I + \frac{b-a}{2^m}(\Phi(\Delta_{m,j}) - I) \tag{26}$$

$$\Psi(b, a) \approx \frac{b-a}{2^m}(\Psi(\Delta_{m,j})) \tag{27}$$

Since $(t_0, t_0') \subseteq \Delta_{m,j}$ for some j and similar for (t_f', t_f), we employ the above approximations. As the entrywise error is quadratic from a linear interpolation, the infinity-norm of the error in Φ and the induced infinity-norm of Ψ ($\max_i \sum_{j,k} |\Psi^i_{j,k}|$) also behave quadratically in time. As a result, any norm of the errors in these tensors behaves quadratically as a result of the equivalence of finite dimensional norms.

With approximations for $\Phi(t_f, t_0)$ and $\Psi(t_f, t_0)$ obtained in $\mathcal{O}(mn^3)$ and $\mathcal{O}(mn^4)$ operations, respectively (due to matrix and tensor multiplication in the cocycle equations), we may solve equation 20 with cost dominated by a single solution of an n dimensional linear system with $\mathcal{O}(n^3)$ complexity. Any future boundary value problems with the same boundary times can be solved in $\mathcal{O}(n^2)$ time as long as the relevant LU factorization is stored from the first solution of equation 20. The estimate of the performance metric in equation 22 also only requires $\mathcal{O}(n^2)$ operations.

APPLICATIONS

The equations of motion for the circular restricted three body problem are given in the synodic frame as

$$\mathbf{F}(\mathbf{x}) = \begin{bmatrix} \dot{x} \\ \dot{y} \\ \dot{z} \\ 2\dot{y} + \frac{\partial \overline{U}}{\partial x} + u_x \\ -2\dot{x} + \frac{\partial \overline{U}}{\partial y} + u_y \\ \frac{\partial \overline{U}}{\partial z} + u_z \end{bmatrix} \tag{28}$$

where the state vector is $\mathbf{x} = [x, y, z, \dot{x}, \dot{y}, \dot{z}]^T$, $\mathbf{u} = [u_x, u_y, u_z]^T$ denotes the control acceleration, an over dot denotes time derivative, and $\overline{U}(x, y, z) = \frac{1-\mu^*}{||\mathbf{r}_1||} + \frac{\mu^*}{||\mathbf{r}_2||} + \frac{x^2+y^2}{2}$ is the effective potential given the reduced mass $\mu^* = \frac{m_2}{m_1+m_2}$ for the two primary bodies with mass m_1, m_2 located along the x-axis at $[-\mu^*, 0, 0]$ and $[1-\mu^*, 0, 0]$ with respect to their common barycenter at the origin. $\mathbf{r}_1, \mathbf{r}_2$ give the position of the satellite of interest with respect to the two primary bodies respectively.[1]

We present an example around a Sun-Earth L2 Halo orbit with initial out-of-plane position of 986,000 km shown in canonical units in figure 2. We show the cost for a deputy satellite to rendezvous with the reference orbit after two weeks when the deputy begins on a 10,000km radius sphere centered at the reference orbit initial position with the same rotating frame velocity as the reference satellite.

The control cost J from equation 14 is given in figure 3, where initial position on the sphere is parameterized by the ecliptic angle from the x-axis counterclockwise θ and the out-of-plane angle ϕ from the ecliptic. This figure takes less than a second to generate using the second order approximation to the initial costate solution and the second order approximation to the cost J. We see that the optimal control cost varies by about 25% of its maximum value depending on the initial location, with lowest cost starting relative positions roughly orthogonal to the reference orbit to Sun vector. This is an interesting takeaway that can be found in almost no computation time at all; however, we are more interested in the methodology and how it performs.

Figure 4 shows the error in the final position in kilometers of the deputy satellite given the control derived in two different ways: first, by solving for a second order approximation in equation 24 using Newton's method, and second by the first order approximation in equation 20. These errors

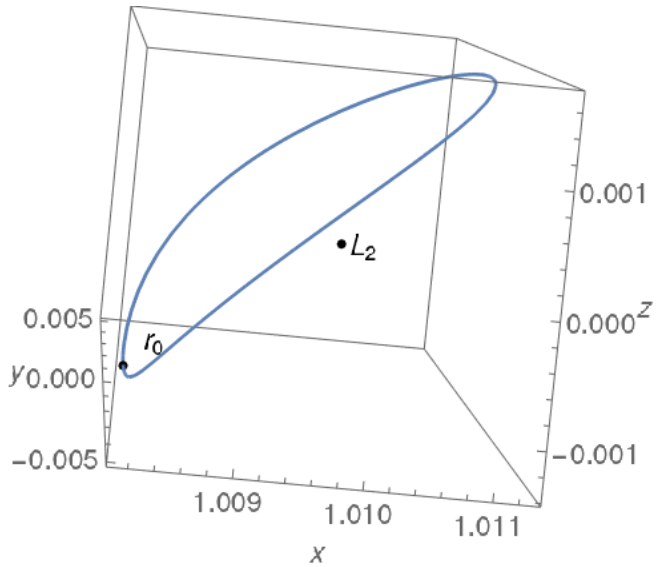

Figure 2: The reference Sun-Earth L2 Halo orbit in canonical distance units.

are calculated by direct numerical integration of the initial states and costates calculated by the two approximation methods. Errors in the final position are on the order of $0.01, 0.1\%$ of the distance traversed for the second order and first order approximations respectively. In simulations below 1,000km distances, negligible difference in the position error between the two approximations is achieved, while the error from the linear approximation varies linearly with the distance. As relative distances increase beyond 10,000km and exceed 100,000km, the final position error blows up quickly as the approximated optimal control problem becomes increasingly far removed from the actual optimal control problem.

Figure 3 also shows that errors in the estimated control cost from equation 22 are on the order of 0.1% percent of the actual cost computed by numerical integration along the approximately computed trajectory. This means that the second order state transition tensor gives a reliable indicator of the performance metric of the optimal control that we can calculate without online numerical integration. Interestingly, the error is zero seemingly along a great circle on the sphere of initial locations of the deputy satellite. This great circle also happens to correspond to the locations of minimal cost rendezvous.

In the above example with figures 3 and 4, we used exact values of the state transition matrix and state transition tensor without interpolation. Here, we analyze interpolation error in this context to show that the induced 2-norm of the error in Φ and the induced infinity-norm of Ψ ($\max_i \sum_{j,k} |\Psi^i_{j,k}|$) behave quadratically in time as expected. Figure 5 demonstrates the induced norms of the error of $\Phi(t_0 + \Delta t, t_0), \Psi(t_0 + \Delta t, t_0)$ interpolated from a fixed $\Phi(\Delta t, 0), \Psi(\Delta t, 0)$ with $t_0, t_0 + \Delta t \in (0, 1)$ days. Figure 6 gives the same errors in $\Phi(\Delta t/2, 0), \Psi(\Delta t/2, 0)$ while considering a variable Δt for interpolation from $\Phi(\Delta t, 0), \Psi(\Delta t, 0)$ respectively. $\Delta t/2$ is employed as this is where we see the maximum error in figure 5. In both cases, we look at the error in the given norm relative to a fixed quantity: $||\Phi(1, 0)||_2$ or $||\Psi(1, 0)||_\infty$ respectively. Quadratic behavior in time is observed in both contexts, and we conclude that entrywise linear interpolation is a reasonable approach to interpolation of state transition tensors. Note that the saddle like behavior in figure 5 simply indicates that interpolants that share the center of their interval with the state transition

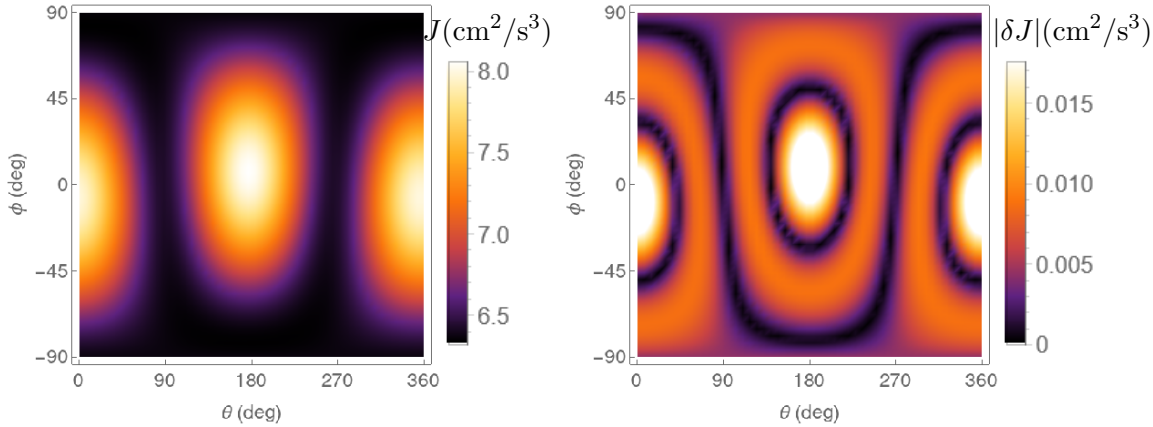

Figure 3: The rendezvous control cost approximated by second order state transition tensor and the error in its approximation versus numerical integration.

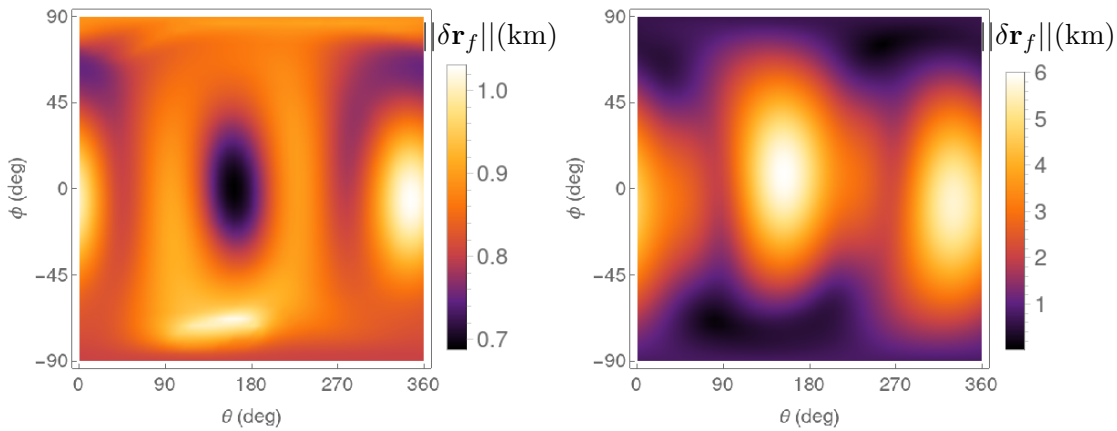

Figure 4: The error in final position due to the approximation of the rendezvous optimal control by second order and first order methods.

tensor they are interpolating are better approximations than interpolants of the same interval length, but different centering.

From this example and the surrounding error analysis, we can conclude that for a discretization with minimum time ranges of one day, any interpolation error norm for Φ and Ψ below this time threshold is less than one part in one thousand and one part in one hundred, respectively. However, the error in norm is not necessarily indicative of the overall performance of the method. To check this, we examine the worst-case error when computing the energy cost J using STTs at the $m = 11$ level of discretization for 5,000 randomly generated transfers from the 10,000 km sphere around the chief satellite to the chief satellite. This test is conducted over time spans from 1 to 30 days. Worst-case error is achieved by employing approximated STTs at the end points of the transfer with exactly half the time span of the finest discretization. We see in figure 7 that error in approximations of cost due to interpolation for 1 to 30 day rendezvous remains below 1 percent of the actual value of the maneuver cost. This is 100 times the size of the error in STT norm as predicted for the $m = 11$ level by figure 6. Such a discrepancy indicates that computations may rely on portions of the STT

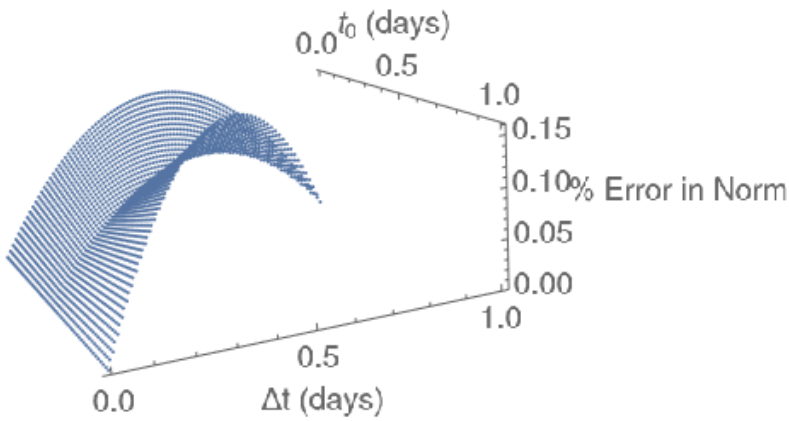

Figure 5: Error 2-norm for the state transition matrix $\Phi(t_0+\Delta t, t_0)$ interpolated from $\Phi(1,0)$ versus the exact value of $\Phi(t_0 + \Delta t, t_0)$. Percentage is calculated by comparison to norm of $\Phi(1,0)$, the state transition matrix over a one day time period. The plot for the infinity norm of the state transition tensor gives the same plot scaled up by approximately one order of magnitude.

for which absolute errors are small compared to the largest components of the STT, but are larger when compared to just the relevant components for a given calculation. The bias observed in figure 7, as well as the poor performance in actual computation versus norm of the error, suggest that a better interpolation scheme may be beneficial. However, the nominal 1% effect of the error at the scale of single-day transfers may not be problematic, and fidelity may be tuned to desired levels by refining the discretization. For example, reducing the discretization order m by one results in a quadrupling of the absolute error. Accuracy needs will vary by application, but discretizations with minimum times around one tenth of one day or $m = 11$ are reasonable in the approximately 1 percent error created during interpolation. Any reduction in this error will be balanced by increased memory costs and very small increases in online computational costs due to the number of matrix multiplications required to form the state transition tensors from precomputed components.

CONCLUSION

We have presented an algorithm for solving any continuous thrust energy-optimal relative transfer sufficiently close to a given reference trajectory regardless of boundary times or values. Our treatment is agnostic of the specific dynamical system, and the choice of reference orbit; however, 'sufficiently close' amounts to deviations approximately 1 percent of the extent of the reference orbit in the Sun-Earth L2 Halo orbit cases tested. The algorithm requires on the order of megabytes of memory for precomputed variational data in nominal Sun-Earth L2 Halo orbit cases tested, and requires only a small number of matrix/tensor multiplications and solutions of linear systems during the online segment of the algorithm. Importantly, there are no numerical solutions of either ordinary or partial differential equations during the online segment of the algorithm. This leads to fast approximation of solutions which may enable the solution of future problems involving nested optimizations. Starshade observation schedule optimization for exoplanet direct imaging missions is one such application in which a doubly nested optimization could be necessary. For this application or others, it is important to validate that solutions to the unconstrained optimal control problem do not violate operational constraints on thrust magnitude. Error analysis dependent on the extent of the relative motion in the given system is also important to assure that this algorithm can reasonably

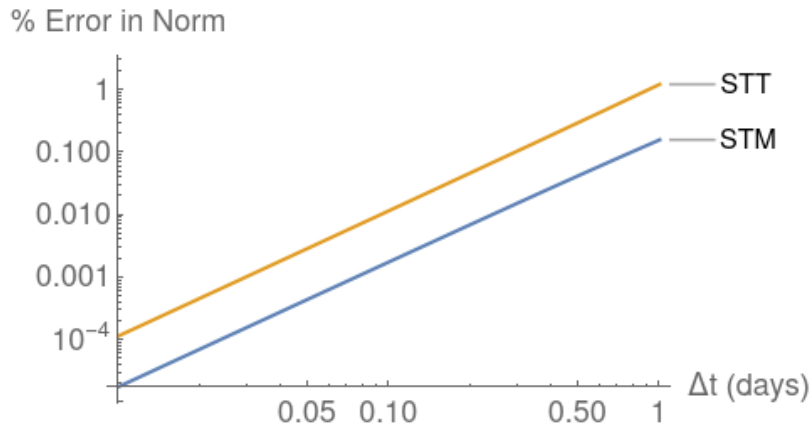

Figure 6: Worst case interpolation error norm for the state transition matrix and second order state transition tensor with respect to the norm of $\Phi(1,0)$ and $\Psi(1,0)$. Interpolation is from state transition tensors beginning at zero and with time span (Δt).

be applied in a given situation with either linear or second order approximations.

A drawback in this method is that only control that is locally optimal about the reference trajectory is considered and the globally optimal control may not be described by the variational equations. This merits further investigation. Some of this methodology will also fail when the sensitivity of states to costates is singular along a given reference trajectory. Given the use of second order variational equations, it should be possible to remedy this issue with special care taken in the numerical solution process of the second order approximation to the solution of the boundary value problem.

A fundamental limit of this method is its inability to be applied to fuel optimal control problems which lack the requisite smoothness and under which uncontrolled trajectories are singular in some variational sense. Instead, the energy optimal control from this method can be used in place of the fuel optimal control, or as a quickly computed initial guess for another scheme to compute the fuel optimal control. However, the fuel costs of the energy optimal solution can be calculated or approximated in a number of ways, from bounding inequalities to numerical integration of the optimal control trajectory. Fast approximation of fuel use with a simple quadrature rule and the precomputed solutions to the variational equations for the costates corresponding to the control over time is slated for future study.

ACKNOWLEDGMENTS

The authors would like to thank the Department of Defense for its generous support through the NDSEG fellowship as well as Nick Oetting for helpful discussions.

REFERENCES

[1] E. Kolemen and N. J. Kasdin, "Optimization of an occulter-based extrasolar-planet-imaging mission," *Journal of guidance, control, and dynamics*, Vol. 35, No. 1, 2012, pp. 172–185.

[2] G. J. Soto, D. Savransky, D. Garrett, and C. Delacroix, "Parameterizing the search space of starshade fuel costs for optimal observation schedules," *Journal of Guidance, Control, and Dynamics*, Vol. 42, No. 12, 2019, pp. 2671–2676.

[3] T. N. Edelbaum, "Optimum low-thrust rendezvous and station keeping," *AIAA Journal*, Vol. 2, No. 7, 1964, pp. 1196–1201.

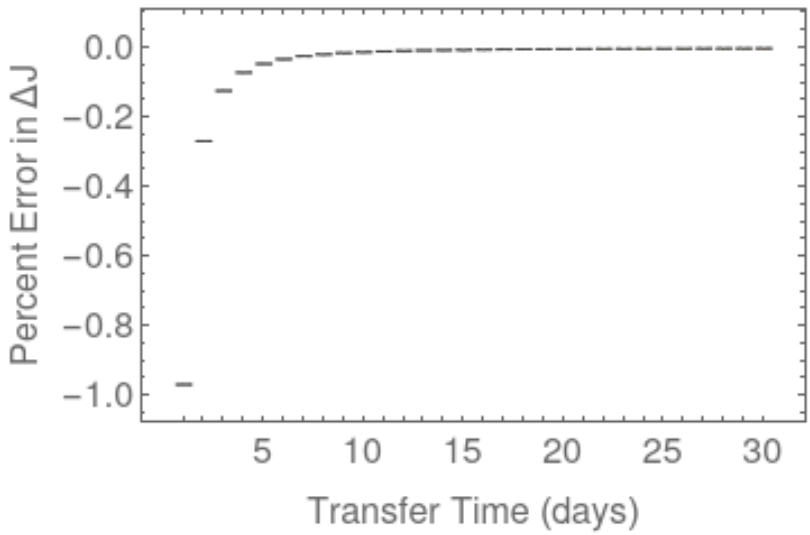

Figure 7: Distribution plot of 5000 random initial conditions on the 10,000km sphere rendezvousing with the chief at the center. Spread of each distribution in cost error is dwarfed by the bias towards overestimating the energy loss from the maneuver. This leaves the distributions to appear almost as points at the given scaling. The error in cost due to the interpolation is below 1% for the given value of $m = 11$ when transfer times are at least 1 day. This relative error decreases with longer transfer times.

[4] T. Carter and M. Humi, "Fuel-optimal rendezvous near a point in general Keplerian orbit," *Journal of Guidance, Control, and Dynamics*, Vol. 10, No. 6, 1987, pp. 567–573.

[5] T. E. Carter, "New form for the optimal rendezvous equations near a Keplerian orbit," *Journal of Guidance, Control, and Dynamics*, Vol. 13, No. 1, 1990, pp. 183–186.

[6] T. Carter and J. Brient, "Optimal bounded-thrust space trajectories based on linear equations," *Journal of optimization theory and applications*, Vol. 70, No. 2, 1991, pp. 299–317.

[7] T. Carter and J. Brient, "Fuel-optimal rendezvous for linearized equations of motion," *Journal of Guidance, Control, and Dynamics*, Vol. 15, No. 6, 1992, pp. 1411–1416.

[8] T. E. Carter and C. J. Pardis, "Optimal power-limited rendezvous with upper and lower bounds on thrust," *Journal of Guidance, Control, and Dynamics*, Vol. 19, No. 5, 1996, pp. 1124–1133.

[9] C. A. Lembeck and J. E. Prussing, "Optimal impulsive intercept with low-thrust rendezvous return," *Journal of guidance, control, and dynamics*, Vol. 16, No. 3, 1993, pp. 426–433.

[10] I. Elliott and N. Bosanac, "Impulsive Control of Formations near Invariant Tori via Local Toroidal Coordinates," *AAS/AIAA Astrodynamics Specialist Conference*, 2021.

[11] K. C. Howell and B. T. Barden, "Trajectory design and stationkeeping for multiple spacecraft in formation near the Sun-Earth L1 point," *IAF 50th International Astronautical Congress*, 1999, pp. 4–8.

[12] K. C. Howell and B. G. Marchand, "Natural and non-natural spacecraft formations near the L1 and L2 libration points in the Sun–Earth/Moon ephemeris system," *Dynamical Systems*, Vol. 20, No. 1, 2005, pp. 149–173.

[13] H. J. Pernicka, B. A. Carlson, and S. Balakrishnan, "Spacecraft formation flight about libration points using impulsive maneuvering," *Journal of guidance, control, and dynamics*, Vol. 29, No. 5, 2006, pp. 1122–1130.

[14] G. Franzini, M. Innocenti, and M. Casasco, "An adjoint-based method for continuous-thrust relative maneuver computation in the restricted three-body problem," *2021 American Control Conference (ACC)*, IEEE, 2021, pp. 4276–4281.

[15] C. Park, V. Guibout, and D. J. Scheeres, "Solving optimal continuous thrust rendezvous problems with generating functions," *Journal of Guidance, Control, and Dynamics*, Vol. 29, No. 2, 2006, pp. 321–331.

[16] S. Boone and J. Mcmahon, "Rapid Local Trajectory Optimization Using Higher-Order State Transition Tensors and Differential Dynamic Programming," 08 2020.

[17] S. Boone and J. McMahon, "Orbital Guidance Using Higher-Order State Transition Tensors," *Journal of Guidance, Control, and Dynamics*, Vol. 44, No. 3, 2021, pp. 493–504.

[18] S. Boone and J. McMahon, "Variable Time-of-Flight Spacecraft Maneuver Targeting Using State Transition Tensors," *Journal of Guidance, Control, and Dynamics*, Vol. 44, No. 11, 2021, pp. 2072–2080.

[19] J. Kulik and D. Savransky, "Precomputation and interpolation of the matrizant for starshade slewing," *Space Telescopes and Instrumentation 2022: Optical, Infrared, and Millimeter Wave*, SPIE, 2022.

[20] H. Rein and D. Tamayo, "Second-order variational equations for N-body simulations," *Monthly Notices of the Royal Astronomical Society*, Vol. 459, No. 3, 2016, pp. 2275–2285.

[21] M. Majji, J. L. Junkins, and J. D. Turner, "A high order method for estimation of dynamic systems," *The Journal of the Astronautical Sciences*, Vol. 56, No. 3, 2008, pp. 401–440.

[22] A. Bani Younes, "Exact Computation of High-Order State Transition Tensors for Perturbed Orbital Motion," *Journal of Guidance, Control, and Dynamics*, Vol. 42, No. 6, 2019, pp. 1365–1371.

[23] A. E. Bryson and Y.-C. Ho, *Applied optimal control: optimization, estimation, and control*. Routledge, 2018.

[24] S. Boone and J. Mcmahon, "Directional State Transition Tensors for Capturing Dominant Nonlinear Dynamical Effects," 08 2021.

[25] J. D. Hadjidemetriou, "Some properties of the solution of the first-order variational equations of the restricted three-body problem," *The Astronomical Journal*, Vol. 72, 1967, p. 865.